Original Research Article

Forecasting Oil Production and Consumption Using the Time-delayed Fractional Discrete Grey Model with Multiple Fractional Order

Abstract

Accurate production and consumption forecasts play a crucial role in economic development, environmental protection, and market investment. By introducing fractional accumulation and time delay effects, the time-delayed fractional discrete grey model with multiple fractional order can more accurately capture the dynamic changes in data. The versatility and flexibility of this model allow it to adapt to various data characteristics and complexities, thereby providing higher forecasting accuracy compared to traditional grey models. Therefore, this study employs the existing time-delayed fractional discrete grey model with multiple fractional order and combines it with the Particle Swarm Optimization algorithm to optimize the fractional order. Experimental results show that the model demonstrates significant advantages in both fitting and forecasting capabilities. Through an in-depth analysis of oil production and consumption data in the Asia-Pacific region, the Commonwealth of Independent States (CIS), and the Middle East, this study proves the prediction accuracy and reliability of the TDF-DGM model in these regions. These results not only provide new insights for research in related fields but also offer valuable references for policymakers and investors.

keywords: time-delayed; grey model; fractional order; oil production and consumption

1 Introduction

Predicting oil production and consumption holds significant strategic importance. Firstly, oil production and consumption, as one of the most crucial global energy sources, directly impact the economic development of countries and regions. For oil-exporting countries, production forecasts help optimize extraction plans and maximize economic benefits. For importing countries, consumption forecasts assist in formulating import plans, thereby avoiding economic fluctuations caused by supply shortfalls. Secondly, oil production and consumption have substantial environmental impact. Predicting oil production and consumption can help governments and environmental agencies assess future carbon emissions and formulate corresponding emission reduction policies and measures. Moreover, accurate production and consumption forecasts provide vital information

to market participants, aiding them in making informed investment and trading decisions, thereby reducing market uncertainties.

The grey prediction model is a method used for time series analysis and forecasting, particularly suitable for small samples and uncertain systems. It falls under the scope of grey system theory, proposed by Chinese scholar Deng in 1982 [1]. The main characteristics of the grey prediction model include applicability to small samples, handling of uncertainty and simplicity. The grey prediction model mainly includes the GM(1, 1) model, where "1, 1" denotes a first-order univariate time series model. The primary modeling steps involve constructing the original data sequence, generating an accumulated generating operation(AGO) sequence, constructing the grey differential equation, parameter estimation, generating predictions and restoring predicted values. The generation of sequences and the structure of the model are the most significant differences compared to other prediction models. The grey prediction model is widely applied in various fields, such as economic forecasting, population forecasting, energy consumption forecasting and environmental change forecasting.

In 2009, Xie and Liu [2, 3, 4] proposed the DGM(1,1) model. In 2013, Wu *et al*. [5] introduced the FGM(1, 1) model. Additionally, researchers have developed various other grey prediction models, such as NDGM(1, 1) [6], DDGM(1, 1) [7], SADGM(1, 1) [8], TDPGM(1, 1) [9], UGM(1, 1) [10], and KRNGM(1, 1) [11], etc. The emergence of these models demonstrates the diversity of grey system theory in addressing forecasting challenges. However, due to the complexity of real-world phenomena, the limitations of these models in handling nonlinear data have gradually become apparent as research has progressed. To better describe this complexity, a multitude of nonlinear grey models have been proposed, such as the Grey Verhulst model [12], Grey NGM$(1, 1, \gamma)$ model [13], Grey NGBM(1, 1) model [14], Time-varying Grey Power model [15], and Grey Lokta-Volterra model [16]. Building on this foundation, 2020 saw the introduction of further models, including the Generalized Grey Verhulst model [17], Grey Riccati-Bernoulli model [18], Grey NBGM$(1, 1, t^{\alpha})$ model [19] and Grey Riccati model[20, 21].

Wu *et al*. [22] were the first to introduce fractional order into grey models. Their examples demonstrated that fractional grey models have higher accuracy than classical models, allowing for more precise predictions of real-world problems. Subsequently, many scholars have made improvements and conducted further research on fractional grey prediction models. In 2019, Wu *et al*. [23] proposed a new fractional accumulated nonlinear grey Bernoulli model (FANGBM(1, 1)). Results showed that the FANGBM(1, 1) model achieves high accuracy in various situations. Hu *et al*. [24] developed a time-delayed fractional grey model with multiple fractional order to predict natural gas consumption, considering the delay effect. Theoretical analysis indicated that this model offers a more general representation, unbiasedness, and greater flexibility compared to existing similar models. Prediction results showed that this model significantly outperformed other comparative grey models. These studies fully demonstrate the role of fractional order and time-delay terms in enhancing the accuracy of grey model predictions, providing higher flexibility and precision in modeling.

The time-delayed fractional grey model with multiple fractional order (TDF-DGM), by incorporating fractional order accumulation and time-delay effects, can more accurately capture the dynamic changes in data, thus providing higher prediction accuracy compared to traditional grey

models. Moreover, this model effectively addresses the time-delay effects in data, describing the lag in system changes and enhancing prediction accuracy. Its generality and flexibility allow it to adapt to different types of data characteristics and complexities. The model demonstrates higher predictive accuracy and stability in practical applications, particularly in handling nonlinear data, thereby improving the reliability and accuracy of predictions. Therefore, this paper chooses to use the TDF-DGM model proposed by Hu [24] to forecast oil production and consumption in the Asia Pacific, the CIS and the Middle East regions.

The rest of this article is arranged as follows. In Section 2, the prediction model and the fractional order optimization method are introduced respectively. In Section 3, three prediction cases are presented, and conclusions are drawn in Section 4.

2 Research methodology

2.1 The time-delayed fractional discrete grey model with multiple fractional order

From Ref.[24], given an original non-negative sequence $X^{(0)} = (x^{(0)}(1), x^{(0)}(2), \cdots, x^{(0)}(n))$, its r_1-order accumulation sequence is $X^{(r_1)} = (x^{(r_1)}(1), x^{(r_1)}(2), \cdots, x^{(r_1)}(n))$. The time-delayed fractional discrete grey model with multiple fractional order can be expressed as a differential equation,

$$\frac{\mathrm{d}x^{(r_1)}(t)}{\mathrm{d}t} + m_1 x^{(r_1)}(t) = m_2 t^{(r_2)} + m_3, \tag{1}$$

where

$$t^{(r_2)} = \sum_{\eta=1}^{k} \binom{k-\eta+r_2-1}{k-\eta} \eta. \tag{2}$$

Eq.(1) is an extension of the whitening equation derived from the FTDGM(1, 1) model [25], and by differentiating $\frac{\mathrm{d}x^{(r_1)}(t)}{\mathrm{d}t}$, we obtain

$$x^{(r_1)}(k+1) - x^{(r_1)}(k) + m_1 x^{(r_1)}(k) = m_2 k^{(r_2)} + m_3,$$

and it can also be expressed as

$$x^{(r_1)}(k+1) = (1+m_1) x^{(r_1)}(k) + m_2 k^{(r_2)} + m_3. \tag{3}$$

Let $\sigma_1 = 1 + m_1$, $\sigma_2 = m_2$, and $\sigma_3 = m_3$, the basic form of the model is

$$x^{(r_1)}(k+1) = \sigma_1 x^{(r_1)}(k) + \sigma_2 k^{(r_2)} + \sigma_3, k = 2, 3, \cdots, n-1 \tag{4}$$

Given the fractional orders r_1 and r_2, we need to solve for the parameters σ_1, σ_2 and σ_3 using the least squares method

$$u = [\sigma_1, \sigma_2, \sigma_3]^T = (B^T B)^{-1} B^T Y \tag{5}$$

where

$$B = \begin{bmatrix} x^{(r_1)}(2) & 1^{(r_2)} & 1 \\ x^{(r_1)}(3) & 2^{(r_2)} & 1 \\ \vdots & \vdots & \vdots \\ x^{(r_1)}(\xi-1) & (\xi-1)^{(r_2)} & 1 \end{bmatrix}, Y = \begin{bmatrix} x^{(r_1)}(2) \\ x^{(r_1)}(3) \\ \vdots \\ x^{(r_1)}(\xi) \end{bmatrix}, \tag{6}$$

and ξ represents the number of modeling points.

Set initial condition $x^{(r_1)}(1) = x^{(0)}(1)$, and then by recursively solving the Eq.(4), the discrete response function of the model is written as

$$\hat{x}^{(r_1)}(k) = \hat{\sigma}_1^k x^{(0)}(1) + \hat{\sigma}_2 \sum_{i=1}^{k} \hat{\sigma}_1^{k-i} i^{(r_2)} + \frac{1-\hat{\sigma}_1^k}{1-\hat{\sigma}_1}\hat{\sigma}_3, k = 2, \ldots, n-1. \tag{7}$$

Therefore, the restored values $\hat{x}^{(0)}(k)$ can be expressed as

$$\hat{x}^{(0)}(k) = \sum_{\eta=1}^{k} \binom{k-\eta-r_1-1}{k-\eta} \hat{x}^{(r_1)}(\eta). \tag{8}$$

2.2 Fractional order optimization method

The previous section introduces the time-delayed fractional discrete grey model with multiple fractional order. Obviously, the fractional orders r_1 and r_2 affect the prediction ability of the time-delayed fractional discrete grey model with multiple fractional order to a great extent and play an extremely important role in the establishment of the model. Therefore, this section aims to optimize the fractional orders r_1 and r_2.

In this work, we have chosen the Mean Absolute Percentage Error (MAPE) as the primary evaluation metric. Firstly, MAPE, as a relative error metric, offers an intuitive understanding of prediction accuracy since it directly reflects the percentage difference between predicted and actual values. Secondly, MAPE is scale-invariant and unaffected by changes in the scale of the data, making it suitable for datasets with different units or magnitudes. Thirdly, MAPE treats all data points' errors equally, regardless of their magnitude, thus reflecting their relative importance in the overall error. Additionally, compared to other complex error metrics, MAPE is simple to calculate, easy to interpret, and practical for model evaluation and comparison in real-world applications. Therefore, MAPE provides us with a straightforward and effective tool for measuring model prediction performance. The MAPE for both the fitting and prediction stages is represented by the following equation, serving as a comprehensive evaluation of the model's fitting and prediction performance.

$$\mathbf{MAPE}_{fit} = \frac{1}{\xi}\sum_{k=1}^{\xi}\left|\frac{\hat{x}^{(0)}(k) - x^{(0)}(k)}{x^{(0)}(k)}\right| \times 100\%, \tag{9}$$

$$\mathbf{MAPE}_{pred} = \frac{1}{n-\xi}\sum_{k=1}^{n-\xi}\left|\frac{\hat{x}^{(0)}(k) - x^{(0)}(k)}{x^{(0)}(k)}\right| \times 100\%, \tag{10}$$

where ξ represents the number of modeling points.

$$\min J(r) = \frac{1}{\xi}\sum_{k=1}^{\xi}\left|\frac{\hat{x}^{(0)}(k) - x^{(0)}(k)}{x^{(0)}(k)}\right| \times 100\%$$

$$\text{s.t.} \begin{cases} [\sigma_1, \sigma_2, \sigma_3]^T = (B^T B)^{-1} B^T Y \\ B = \begin{pmatrix} x^{(r_1)}(2) & 1^{(r_2)} & 1 \\ x^{(r_1)}(3) & 2^{(r_2)} & 1 \\ \vdots & \vdots & \vdots \\ x^{(r_1)}(\xi-1) & (\xi-1)^{(r_2)} & 1 \end{pmatrix} \\ Y = \begin{pmatrix} x^{(r_1)}(2) & x^{(r_1)}(3) & \cdots & x^{(r_1)}(\xi) \end{pmatrix}^T \\ \hat{x}^{(r_1)}(k) = \hat{\sigma}_1^k x^{(0)}(1) + \hat{\sigma}_2 \sum_{i=1}^{k} \hat{\sigma}_1^{k-i} i^{(r_2)} + \frac{1-\hat{\sigma}_1^k}{1-\hat{\sigma}_1}\hat{\sigma}_3, k = 2, \ldots, n-1 \\ \hat{x}^{(0)}(k) = \sum_{\eta=1}^{k} \binom{k-\eta-r_1-1}{k-\eta} \hat{x}^{(r_1)}(\eta), k = 2, \ldots, n-1 \end{cases}, \tag{11}$$

To solve the aforementioned optimization problem, we employ the Particle Swarm Optimization (PSO) algorithm. PSO is an optimization algorithm inspired by the social behavior of bird flocks. By sharing information among individuals, PSO utilizes both individual and global best experiences within the swarm to iteratively update the positions and velocities of particles, thereby approaching the optimal solution.

The fundamental idea of PSO is to represent each candidate solution as a particle in the search space, and update the particle's position based on its velocity, personal best position, and global best position. The update equations for the velocity and position are

$$\begin{cases} v_i(t+1) = w \cdot v_i(t) + c_1 \cdot r_1 \cdot (p_i - x_i(t)) + c_2 \cdot r_2 \cdot (g - x_i(t)) \\ x_i(t+1) = x_i(t) + v_i(t+1) \end{cases}, \tag{12}$$

where $v_i(t)$ and $x_i(t)$ represent the velocity and position of the i-th particle at time t, respectively. w is the inertia weight, c_1 and c_2 are learning factors. r_1 and r_2 are random numbers uniformly distributed in the range $[0, 1]$. p_i is the personal best position of the i-th particle, and g is the global best position.

Through multiple iterations, the swarm converges towards the optimal solution, thereby finding the global optimum of the optimization problem. PSO is widely used due to its simplicity, ease of parallelization and strong global search capability. In this work, we utilize the PSO algorithm to optimize the model parameters, aiming to minimize the Mean Absolute Percentage Error (MAPE) for both fitting stages.

2.3 Algorithm Steps

To solve the aforementioned optimization problem, we design a solution process based on the Particle Swarm Optimization (PSO) algorithm. The algorithm flow is shown in Algorithm 1. The implementation of this algorithm is based on Python source code and utilizes the pyswarm library. By using the pyswarm library, we can conveniently call the PSO algorithm to optimize the model parameters, thereby minimizing the Mean Absolute Percentage Error (MAPE) for both the fitting stages. For more information and the source code of the pyswarm library, please visit

https://github.com/tisimst/pyswarm.

Algorithm 1: The algorithm for solving the optimization problem

input : The initial sequence $x^{(0)} = \left(x^{(0)}(1), x^{(0)}(2), \ldots, x^{(0)}(n)\right)$, the number of modeling points ξ.

output: The fractional order (r^*)

Set max iteration = 100
Initialize $(\text{MAPE}_{fit})_{\min} = \inf$, the best agent of r
for r in agent, len = max iteration **do**
    Construst B and Y by the Eq.(6)
    Compute $\sigma_1, \sigma_2, \sigma_3$ by the Eq.(5)
    for $k = 1$ to n, step $= 1$ **do**
        Compute $\hat{x}^{(r)}(k)$ by the Eq.(7)
        Compute $\hat{x}^{(0)}(k)$ by the Eq.(8)
    end
    Compute MAPE_{fit} using the objective function in Eq.(9)
    if $\text{MAPE}_{fit} < (\text{MAPE}_{fit})_{\min}$ **then**
        $(\text{MAPE}_{fit})_{\min} \leftarrow \text{MAPE}_{fit}$
        $r^* \leftarrow r$
    end
end

3 Applications in forecasting oil production and consumption

Predicting oil production and consumption trends in the Asia Pacific, CIS (Commonwealth of Independent States) and the Middle East is crucial for the stability of the global energy market and economic development. These regions are key players in global oil production and consumption, significantly influencing the balance of supply and demand and the stability of oil prices worldwide. Accurate forecasts of production and consumption trends in these areas enable governments and businesses to formulate effective energy policies and strategies, ensuring market stability, reducing risks, and fostering economic growth. Additionally, these predictions aid in energy security, investment decisions, environmental protection, and geopolitical strategy formulation, providing essential information to support the healthy and sustainable development of the global energy market.

We have gathered annual data on oil production and consumption for the Asia Pacific, CIS (Commonwealth of Independent States) and the Middle East, spanning the years 2000 to 2022. The dataset from 2000 to 2015 has been utilized to build the forecasting model. and the data from 2016 to 2022 has been reserved for out-of-sample testing to evaluate the model's generalization capability effectively. This approach allows for a more comprehensive assessment of the model's ability to predict future trends.

To evaluate the effectiveness of the time-delayed fractional grey model with multiple fractional order, a comprehensive performance comparison was conducted using eight established benchmark grey system models. The details of these benchmark models are provided in Table 1. Additionally, models incorporating external input parameters were optimized using the Particle Swarm Opti-

mization (PSO) algorithm.

Table 1. Benchmark models.

Model	Year	Reference
The classical grey model (GM(1, 1))	1982	[1]
The discrete grey model (DGM(1, 1))	2009	[26]
The nonlinear grey Bernoulli model (NGBM(1, 1))	2008	[27]
The fractional-order grey model (FGM(1, 1))	2013	[22]
The fractional nonlinear grey Bernoulli model (FANGBM(1, 1))	2019	[23]
The fractional order discrete grey model (FDGM(1, 1))	2018	[28]
The fractional grey model (FAGM$(1, 1, t^{\alpha})$)	2019	[29]
The Simpson fractional grey model (SFAGM(1, 1))	2021	[30]

3.1 Case I: Forecasting oil production in the Asia Pacific.

Using oil production data from the Asia Pacific region from 2000 to 2022, the data from 2000 to 2015 is used to construct the grey model, while data from 2016 to 2022 is used to test its out-of-sample performance. Figure 3 shows all the predicted values of the total oil production in this region. Figure 2 presents the main errors in the model predictions and compares them. Table 2 lists the detailed results of the model predictions. In this process, the Particle Swarm Optimization (PSO) algorithm is used to optimize the parameters of eight models, with the optimization results shown in Figure 1.

In this case study, we compare the performance of different models in forecasting a certain time series data. Specifically, we examine the GM$(1,1)$, DGM$(1,1)$, NGBM$(1,1)$, FGM$(1,1)$, FANGBM$(1,1)$, FDGM$(1,1)$, FAGM$(1,1,t^{\alpha})$, SFAGM$(1,1)$ and TDF-DGM models and their prediction results. Table 2 provides a detailed comparison of each model's predicted values and actual values at various time points, as well as the corresponding errors.

By analyzing the Mean Absolute Percentage Error for fitting (MAPE$_{fit}$) and the Mean Absolute Percentage Error for prediction (MAPE$_{pre}$) of each model, it can be found that the TDF-DGM model exhibits the best overall performance. Its MAPE$_{fit}$ value is 0.7173%, and its MAPE$_{pre}$ value is 3.0892%, both lower than those of the other models. This indicates that the TDF-DGM model not only excels in fitting the data but also has a high accuracy in predicting future data.

The data in Table 2 further reveals the performance of different models at specific time points. For instance, in the second row of Table 2, the predicted value of the NGBM(1,1) model matches the original data perfectly. However, in the 22nd row of Table 2, the prediction errors of all models are relatively large, with the TDF-DGM model having an error of 1151.85. Despite this, the TDF-DGM model still demonstrates its superior overall performance. The TDF-DGM model outperforms other models in both fitting and prediction performance, particularly in terms of lower prediction errors. Therefore, the TDF-DGM model has a significant advantage in applications requiring high-precision forecasts. However, in practical applications, researchers need to consider the specific data characteristics and application requirements comprehensively, taking into account both the overall performance of the model and its performance at individual time points, to select the most suitable prediction model.

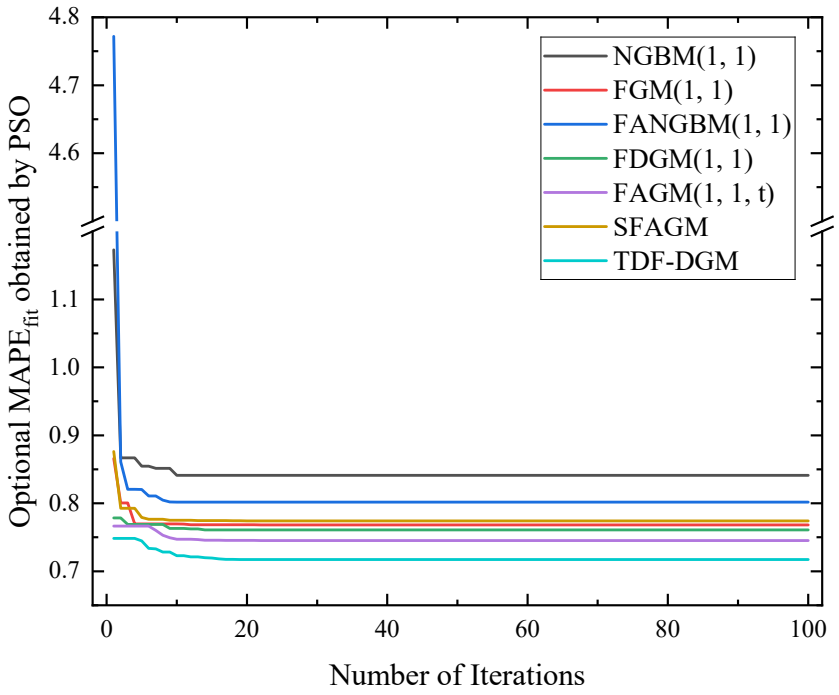

Figure 1. Optimal MAPE$_{fit}$ of model in Case I under PSO algorithm.

Table 2. Detailed results in Case I.

	original data	GM(1, 1)		DGM(1, 1)		NGBM(1, 1)		FGM(1, 1)		FANGBM(1, 1)		FDGM(1, 1)		FAGM(1, 1, t^α)		SFAGM(1, 1)		TDF-DGM	
		value	error	value	error	value	error	value	error	value	error	value	error	value	error	value	error	value	error
1	7879.74	7879.74	0.00	7879.74	0.00	7879.74	0.00	7879.74	0.00	7879.74	0.00	7879.74	0.00	7879.74	0.00	7879.74	0.00	7879.74	0.00
2	7828.73	7781.73	-47.00	7781.96	-46.77	7828.73	0.00	7828.73	0.00	7828.73	0.00	7815.03	-13.70	7828.73	0.00	7828.73	0.00	7860.86	32.13
3	7864.32	7826.24	-38.07	7826.44	-37.87	7841.40	-22.91	7841.93	-22.39	7835.75	-28.57	7823.30	-41.02	7811.32	-53.00	7843.38	-20.94	7802.96	-61.35
4	7789.05	7871.01	81.96	7871.18	82.13	7869.69	80.64	7873.97	84.92	7866.75	77.70	7847.72	58.67	7823.86	34.81	7876.67	87.62	7813.67	24.62
5	7855.81	7916.04	60.23	7916.18	60.38	7905.52	49.71	7913.88	58.08	7905.47	49.67	7880.16	24.36	7855.81	0.00	7917.27	61.47	7855.81	0.00
6	7991.11	7961.32	-29.79	7961.44	-29.67	7945.91	-45.19	7957.39	-33.72	7947.49	-43.62	7917.36	-73.75	7899.73	-91.38	7960.85	-30.26	7914.77	-76.34
7	7938.29	8006.86	68.57	8006.95	68.66	7989.44	51.15	8002.43	64.14	7991.20	52.92	7957.71	19.42	7950.65	12.36	8005.34	67.05	7982.70	44.41
8	7974.96	8052.66	77.70	8052.72	77.76	8035.30	60.34	8047.89	72.93	8035.96	61.00	8000.27	25.31	8005.27	30.31	8049.64	74.68	8054.34	79.38
9	8105.67	8098.73	-6.95	8098.76	-6.92	8082.99	-22.69	8093.11	-12.56	8081.43	-24.25	8044.48	-61.19	8061.34	-44.33	8093.13	-12.54	8125.60	19.93
10	8089.97	8145.05	55.08	8145.05	55.08	8132.19	42.22	8137.69	47.72	8127.45	37.48	8089.97	0.00	8117.38	27.41	8135.45	45.48	8192.88	102.91
11	8456.37	8191.65	-264.72	8191.62	-264.75	8182.68	-273.69	8181.37	-275.00	8173.94	-282.43	8136.46	-319.90	8172.39	-283.98	8176.38	-279.99	8252.76	-203.61
12	8311.41	8238.51	-72.90	8238.45	-72.96	8234.29	-77.11	8223.99	-87.42	8220.84	-90.57	8183.77	-127.64	8225.73	-85.68	8215.80	-95.61	8301.86	-9.55
13	8397.12	8285.63	-111.49	8285.54	-111.58	8286.91	-110.21	8265.43	-131.69	8268.13	-128.99	8231.76	-165.36	8277.01	-120.11	8253.65	-143.48	8336.73	-60.39
14	8253.54	8333.03	79.49	8332.91	79.37	8340.45	86.91	8305.65	52.11	8315.79	62.25	8280.31	26.77	8326.02	72.48	8289.90	36.36	8353.75	100.21
15	8284.09	8380.70	96.61	8380.55	96.46	8394.83	110.74	8344.60	60.51	8363.80	79.72	8329.34	45.25	8372.65	88.56	8324.55	40.47	8349.15	65.07
16	8377.58	8428.64	51.06	8428.45	50.87	8450.00	72.42	8382.27	4.69	8412.18	34.60	8378.78	1.20	8416.88	39.30	8357.64	-19.95	8318.93	-58.65
MAPE$_{fit}$			0.8722		0.8719		0.8412		0.7683		0.8017		0.7608		0.7451		0.7742		**0.7173**
17	8050.82	8476.85	426.03	8476.64	425.82	8505.91	455.09	8418.66	367.84	8460.90	410.08	8428.58	377.76	8458.75	407.93	8389.18	338.35	8258.87	208.05
18	7773.99	8525.35	751.35	8525.10	751.11	8562.54	788.55	8453.79	679.80	8509.99	735.99	8478.69	704.70	8498.34	724.35	8419.22	645.23	8164.49	390.50
19	7632.33	8574.11	941.79	8573.83	941.51	8619.84	987.52	8487.66	855.33	8559.42	927.10	8529.08	896.75	8535.74	903.42	8447.80	815.47	8031.08	398.75
20	7669.39	8623.16	953.77	8622.84	953.46	8677.81	1008.42	8520.30	850.91	8609.22	939.83	8579.71	910.33	8571.08	901.69	8474.98	805.59	7853.62	184.23
21	7455.79	8672.49	1216.70	8672.14	1216.35	8736.41	1280.62	8551.73	1095.95	8659.37	1203.58	8630.56	1174.78	8604.47	1148.68	8500.80	1045.01	7626.84	171.06
22	7373.46	8722.10	1348.64	8721.71	1348.26	8795.63	1422.18	8581.99	1208.53	8709.89	1336.43	8681.61	1308.15	8636.03	1262.57	8525.31	1151.85	7345.19	-28.27
23	7272.79	8771.99	1499.20	8771.57	1498.78	8855.47	1582.67	8611.11	1338.31	8760.77	1487.98	8732.83	1460.03	8665.89	1393.10	8548.58	1275.78	7002.79	-270.01
MAPE$_{pre}$			13.5651		13.5609		14.3013		12.1580		13.3842		12.9927		12.8090		11.5529		**3.0892**

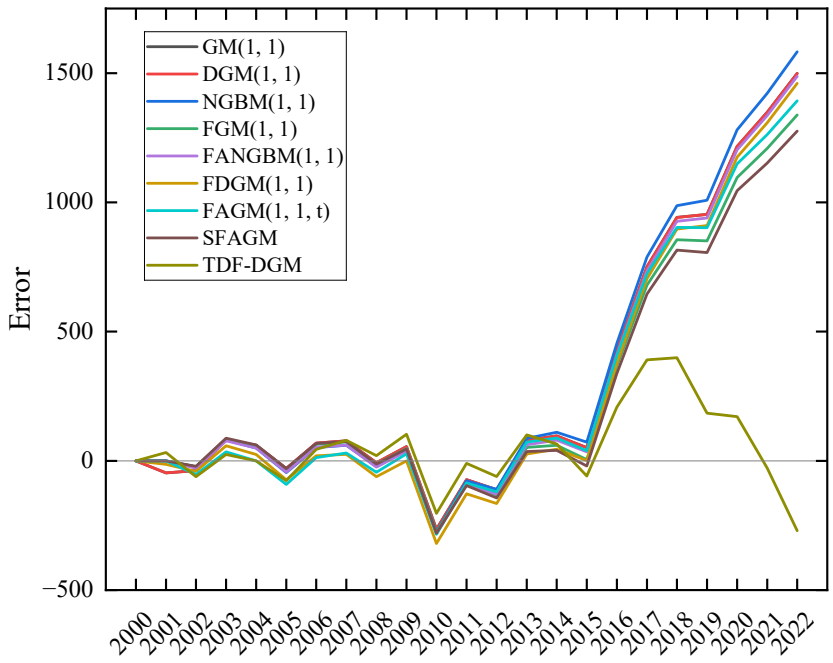

Figure 2. Optimal MAPE_{fit} of model in Case I under PSO algorithm.

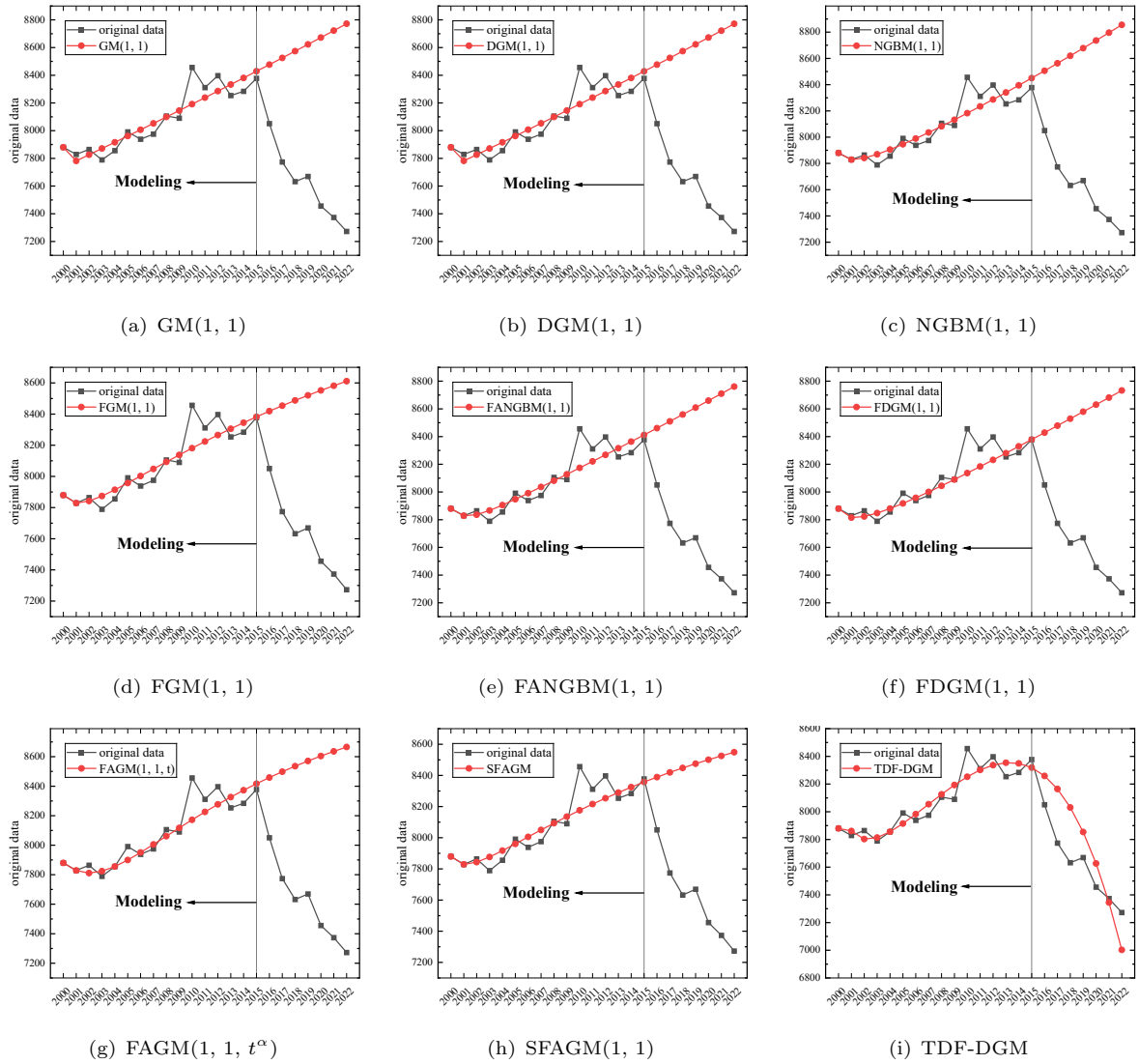

(a) GM(1, 1) (b) DGM(1, 1) (c) NGBM(1, 1)

(d) FGM(1, 1) (e) FANGBM(1, 1) (f) FDGM(1, 1)

(g) FAGM(1, 1, t^{α}) (h) SFAGM(1, 1) (i) TDF-DGM

Figure 3. Predicted values of all models in Case I.

3.2 Case II: Forecasting oil consumption in the CIS.

Using oil production data from the CIS region from 2000 to 2022, the data from 2000 to 2015 is used to construct the grey model, while data from 2016 to 2022 is used to test its out-of-sample performance. Figure 6 shows all the predicted values of the total oil production in this region. Figure 5 presents the main errors in the model predictions and compares them. Table 3 lists the detailed results of the model predictions. In this process, the Particle Swarm Optimization (PSO) algorithm is used to optimize the parameters of eight models, with the optimization results shown in Figure 4.

Table 3 displays the detailed results of different forecasting models in Case II. This table includes the original data as well as the predicted values and errors of the GM(1, 1), DGM(1, 1), NGBM(1, 1), FGM(1, 1), FANGBM(1, 1), FDGM(1, 1), FAGM(1, 1, t^{α}), SFAGM(1, 1) and TDF-DGM models. During the fitting phase, it can be seen from Table 3 that the models perform differently. The fitting performance of each model is evaluated using the Mean Absolute Percentage Error for fitting (MAPE$_{fit}$). The results show that the TDF-DGM model has a MAPE$_{fit}$ value

of 1.8138%, significantly lower than the other models. This indicates that the TDF-DGM model has the smallest error and the best fitting performance. In the prediction phase, the TDF-DGM model once again demonstrates its superior performance. The Mean Absolute Percentage Error for prediction (MAPE_{pre}) shows that the TDF-DGM model has a MAPE_{pre} value of 2.3307%, significantly lower than the other models. This indicates that the TDF-DGM model has the smallest error and the best prediction performance.

Analysis at specific time points reveals several insights. First, in the second row of Table 3, the original data is 3277.20, and the predicted values of the NGBM$(1,1)$ and TDF-DGM models match the original data exactly, with an error of 0.00. In the twelfth row of Table 3, the original data is 3919.24, and all models have negative errors, indicating that the predicted values are lower than the actual values. The FGM$(1,1)$ model has an error of -72.12, while the TDF-DGM model has an error of -52.09. In the twenty-second row of Table 3, the original data is 4438.89, and all models have relatively large errors, especially the FAGM(1,1, t^{α}) model with an error of 579.88, while the TDF-DGM model has an error of 137.34, significantly lower than the other models.

Therefore, the TDF-DGM model demonstrates excellent fitting and prediction capabilities in this case and is recommended for consideration in practical applications. However, different datasets and application scenarios may affect model performance, so it is essential to consider data characteristics and specific requirements comprehensively to select the most suitable prediction model for practical use.

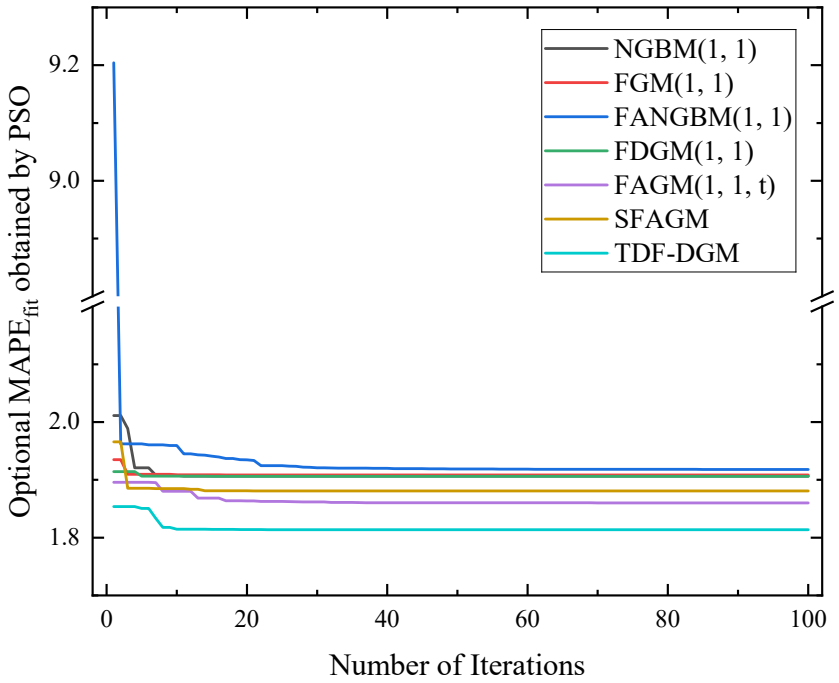

Figure 4. Optimal MAPE_{fit} of model in Case II under PSO algorithm.

Table 3. Detailed results in Case II.

	original data	GM(1, 1)		DGM(1, 1)		NGBM(1, 1)		FGM(1, 1)		FANGBM(1, 1)		FDGM(1, 1)		FAGM(1, 1, t^{α})		SFAGM(1, 1)		TDF-DGM	
		value	error	value	error	value	error	value	error	value	error	value	error	value	error	value	error	value	error
1	3239.03	3239.03	0.00	3239.03	0.00	3239.03	0.00	3239.03	0.00	3239.03	0.00	3239.03	0.00	3239.03	0.00	3239.03	0.00	3239.03	0.00
2	3277.20	3162.92	-114.29	3163.54	-113.66	3277.20	0.00	3277.20	0.00	3277.20	0.00	3277.20	0.00	3295.54	18.33	3277.20	0.00	3277.20	0.00
3	3207.40	3226.69	19.29	3227.26	19.86	3266.49	59.09	3265.60	58.20	3269.49	62.09	3265.94	58.54	3305.24	97.84	3261.53	54.13	3235.63	28.23
4	3357.00	3291.74	-65.25	3292.26	-64.74	3292.97	-64.03	3291.29	-65.71	3297.25	-59.75	3291.78	-65.22	3337.19	-19.81	3286.05	-70.95	3271.14	-85.86
5	3336.31	3358.11	21.80	3358.57	22.26	3337.18	0.88	3335.09	-1.21	3341.91	5.60	3335.66	-0.65	3381.53	45.22	3329.97	-6.34	3331.49	-4.82
6	3357.98	3425.82	67.84	3426.21	68.23	3392.39	34.41	3390.18	32.20	3396.99	39.00	3390.77	32.79	3434.83	76.84	3385.95	27.97	3402.59	44.61
7	3537.85	3494.89	-42.97	3495.22	-42.63	3455.47	-82.38	3453.36	-84.49	3459.53	-78.33	3453.94	-83.92	3495.38	-42.47	3450.56	-87.29	3478.47	-59.38
8	3568.04	3565.35	-2.69	3565.62	-2.42	3524.74	-43.30	3522.89	-45.15	3527.98	-40.06	3523.43	-44.61	3562.23	-5.81	3521.95	-46.09	3556.34	-11.70
9	3634.76	3637.23	2.48	3637.43	2.68	3599.21	-35.54	3597.75	-37.01	3601.43	-33.33	3598.24	-36.52	3634.76	0.00	3599.02	-35.74	3634.76	0.00
10	3498.25	3710.57	212.32	3710.70	212.45	3678.28	180.03	3677.29	179.04	3679.32	181.07	3677.71	179.46	3712.56	214.31	3681.09	182.84	3712.95	214.70
11	3593.41	3785.38	191.97	3785.43	192.02	3761.55	168.13	3761.11	167.70	3761.29	167.88	3761.45	168.04	3795.37	201.96	3767.73	174.32	3790.49	197.08
12	3919.24	3861.70	-57.54	3861.68	-57.56	3848.75	-70.49	3848.93	-70.31	3847.12	-72.12	3849.17	-70.07	3883.02	-36.21	3858.64	-60.60	3867.15	-52.09
13	4069.69	3939.56	-130.13	3939.46	-130.23	3939.72	-129.97	3940.56	-129.13	3936.66	-133.03	3940.69	-128.99	3975.41	-94.28	3953.64	-116.04	3942.80	-126.88
14	4073.13	4018.99	-54.14	4018.80	-54.32	4034.34	-38.79	4035.89	-37.24	4029.81	-43.31	4035.90	-37.22	4072.45	-0.67	4052.61	-20.52	4017.38	-55.74
15	4230.62	4100.02	-130.60	4099.74	-130.87	4132.55	-98.06	4134.85	-95.77	4126.54	-104.08	4134.73	-95.89	4174.14	-56.47	4155.46	-75.15	4090.87	-139.74
16	4107.25	4182.68	75.43	4182.32	75.07	4234.33	127.08	4237.39	130.14	4226.81	119.56	4237.13	129.88	4280.48	173.23	4262.18	154.93	4163.27	56.02
MAPE$_{fit}$			2.0246		2.0251		1.9064		1.9086		1.9181		1.9061		1.8602		1.8809		**1.8138**
17	4201.00	4267.01	66.01	4266.55	65.56	4339.65	138.65	4343.52	142.52	4330.64	129.64	4343.09	142.10	4391.49	190.49	4372.74	171.74	4234.60	33.61
18	4214.42	4353.04	138.62	4352.49	138.06	4448.54	234.11	4453.22	238.80	4438.04	223.62	4452.63	238.21	4507.22	292.79	4487.16	272.74	4304.89	90.47
19	4322.40	4440.80	118.40	4440.15	117.75	4561.01	238.60	4566.53	244.13	4549.06	226.65	4565.76	243.36	4627.72	305.32	4605.47	283.07	4374.16	51.76
20	4387.61	4530.34	142.73	4529.58	141.97	4677.11	289.49	4683.48	295.87	4663.73	276.12	4682.52	294.91	4753.09	365.48	4727.71	340.10	4442.45	54.84
21	4194.20	4621.68	427.48	4620.81	426.61	4796.88	602.68	4804.12	609.92	4782.13	587.93	4802.96	608.76	4883.40	689.20	4853.94	659.74	4509.80	315.60
22	4438.89	4714.86	275.97	4713.88	274.99	4920.39	481.50	4928.50	489.62	4904.31	465.42	4927.12	488.23	5018.77	579.88	4984.23	545.34	4576.23	137.34
23	4627.78	4809.92	182.14	4808.82	181.04	5047.69	419.91	5056.69	428.91	5030.34	402.56	5055.08	427.30	5159.29	531.51	5118.64	490.86	4641.78	14.00
MAPE$_{pre}$			4.4568		4.4393		7.8949		8.0415		7.5900		8.0190		9.6937		9.0688		**2.3307**

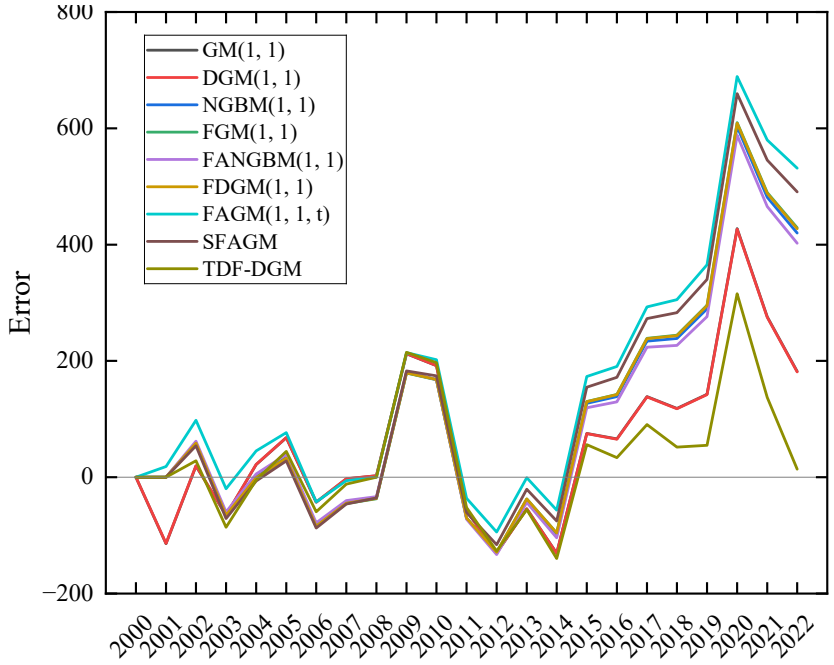

Figure 5. Optimal MAPE$_{fit}$ of model in Case II under PSO algorithm.

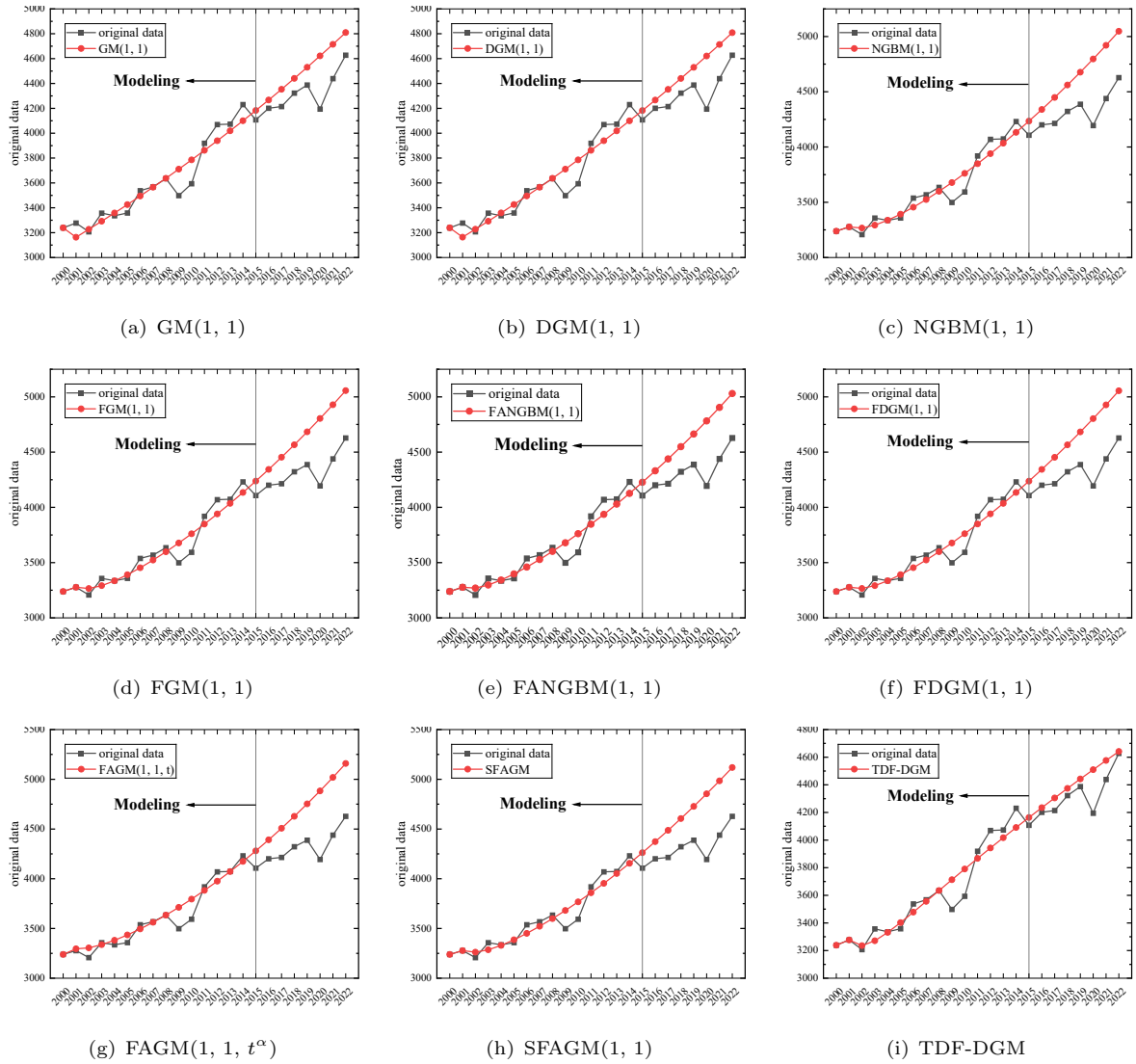

(a) GM(1, 1) (b) DGM(1, 1) (c) NGBM(1, 1)

(d) FGM(1, 1) (e) FANGBM(1, 1) (f) FDGM(1, 1)

(g) FAGM(1, 1, t^{α}) (h) SFAGM(1, 1) (i) TDF-DGM

Figure 6. Predicted values of all models in Case II.

3.3 Case III: Forecasting oil consumption in the Middle East.

Using oil production data from the Middle East region from 2000 to 2022, the data from 2000 to 2015 is used to construct the grey model, while data from 2016 to 2022 is used to test its out-of-sample performance. Figure 9 displays all predicted values of total oil production in the region. Figure 8 illustrates the main errors in model predictions and their comparison. Table 4 provides detailed results of model predictions. Particle Swarm Optimization (PSO) algorithm is employed to optimize parameters of eight models, with optimization results shown in Figure 7.

Table 4 presents detailed results of Case III, covering original data and predictions and errors of various models (GM(1, 1), DGM(1, 1), NGBM(1, 1), FGM(1, 1), FANGBM(1, 1), FDGM(1, 1), FAGM(1, 1, t^{α}), SFAGM(1, 1) and TDF-DGM). Each model's prediction capability is evaluated using Mean Absolute Percentage Error (MAPE), including results from the fitting phase (MAPE$_{fit}$) and prediction phase (MAPE$_{pre}$). Table 4 reveals differences in performance among models during both fitting and prediction phases.

Notably, the TDF-DGM model achieves optimal results in both phases with MAPE metrics.

It shows a MAPE_{fit} of 0.7754% during fitting, indicating the strongest fitting capability to training data. The FAGM$(1, 1, t^{\alpha})$ model follows closely with a fitting error of 0.8120%. In the prediction phase, the TDF-DGM model significantly outperforms other models with a MAPE_{pre} of 4.4986%, demonstrating the strongest predictive capability to unknown data. The FGM$(1, 1)$ model also performs well in the prediction phase with an error of 8.1593%. Specific data points from rows 21 to 23 in Table 4 validate the accuracy of predictions. For instance, in row 21 of Table 4, where the original data is 8245.59, the TDF-DGM model predicts 9358.34 with an error of 1112.76, showing favorable performance. In comparison, the GM(1, 1) model predicts 11358.89 with an error of 3113.31, significantly higher than the TDF-DGM model. Overall, the TDF-DGM model demonstrates superior fitting and prediction capabilities in this case study, suggesting its preference for similar datasets.

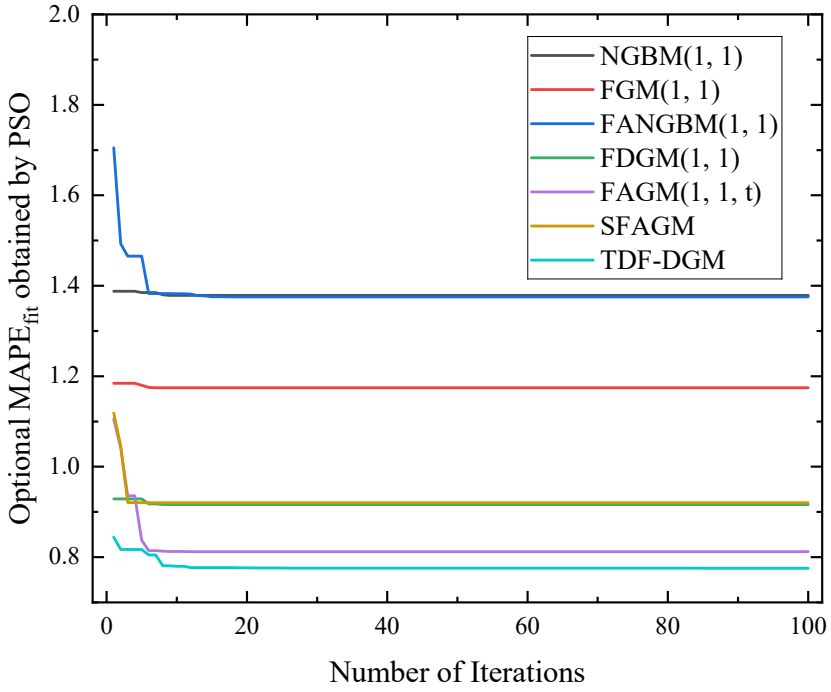

Figure 7. Optimal MAPE_{fit} of model in Case III under PSO algorithm.

Table 4. Detailed results in Case III.

	original data	GM(1, 1)		DGM(1, 1)		NGBM(1, 1)		FGM(1, 1)		FANGBM(1, 1)		FDGM(1, 1)		FAGM(1, 1, t^α)		SFAGM(1, 1)		TDF-DGM	
		value	error	value	error	value	error	value	error	value	error	value	error	value	error	value	error	value	error
1	5022.90	5022.90	0.00	5022.90	0.00	5022.90	0.00	5022.90	0.00	5022.90	0.00	5022.90	0.00	5022.90	0.00	5022.90	0.00	5022.90	0.00
2	5280.14	5368.30	88.16	5369.62	89.48	5017.76	-262.38	5144.79	-135.35	5045.68	-234.46	5257.52	-22.62	5280.14	0.00	5322.94	42.80	5280.14	0.00
3	5425.22	5584.29	159.07	5585.63	160.41	5425.22	0.00	5425.22	0.00	5437.68	12.47	5421.01	-4.21	5404.27	-20.95	5462.50	37.28	5425.43	0.21
4	5614.57	5808.98	194.40	5810.32	195.75	5764.98	150.40	5737.13	122.56	5771.95	157.38	5684.83	70.26	5669.58	55.01	5695.70	81.13	5668.80	54.23
5	5971.27	6042.70	71.43	6044.05	72.78	6072.86	101.59	6053.85	82.59	6076.81	105.54	5996.37	25.10	5973.60	2.33	5987.63	16.36	5953.77	-17.50
6	6365.48	6285.83	-79.65	6287.18	-78.30	6363.53	-1.96	6366.29	0.81	6365.48	0.00	6319.08	-46.40	6288.68	-76.80	6301.58	-63.90	6259.88	-105.60
7	6664.01	6538.74	-125.27	6540.09	-123.92	6644.53	-19.48	6670.69	6.68	6645.06	-18.95	6636.88	-27.13	6604.10	-59.92	6618.47	-45.54	6576.41	-87.60
8	6757.27	6801.83	44.56	6803.18	45.91	6920.31	163.05	6965.40	208.13	6919.79	162.53	6943.89	186.62	6915.03	157.76	6929.91	172.64	6896.35	139.08
9	7238.54	7075.50	-163.03	7076.85	-161.69	7193.74	-44.80	7249.70	11.16	7192.47	-46.07	7238.54	0.00	7219.14	-19.40	7232.64	-5.90	7214.40	-24.14
10	7405.45	7360.19	-45.26	7361.53	-43.92	7466.79	61.35	7523.37	117.92	7465.01	59.56	7520.97	115.52	7515.28	109.83	7525.71	120.26	7526.08	120.63
11	7801.36	7656.33	-145.03	7657.66	-143.69	7740.92	-60.44	7786.45	-14.91	7738.84	-62.52	7791.91	-9.44	7802.91	1.56	7809.12	7.76	7827.29	25.93
12	8119.71	7964.38	-155.33	7965.71	-154.00	8017.22	-102.49	8039.10	-80.61	8015.05	-104.66	8052.26	-67.46	8081.86	-37.85	8083.30	-36.41	8114.13	-5.58
13	8454.73	8284.83	-169.90	8286.14	-168.59	8296.57	-158.15	8281.58	-173.15	8294.50	-160.22	8302.89	-151.83	8352.13	-102.60	8348.81	-105.91	8382.72	-72.01
14	8694.20	8618.17	-76.02	8619.47	-74.73	8579.70	-114.50	8514.19	-180.01	8577.92	-116.28	8544.65	-149.54	8613.82	-80.38	8606.24	-87.95	8629.10	-65.09
15	8922.89	8964.93	42.04	8966.20	43.31	8867.19	-55.70	8737.25	-185.64	8865.90	-56.98	8778.28	-144.61	8867.12	-55.77	8856.16	-66.73	8849.18	-73.71
16	8920.72	9325.63	404.91	9326.88	406.16	9159.59	238.86	8951.09	30.36	9158.98	238.26	9004.44	83.71	9112.23	191.50	9099.10	178.37	9038.68	117.95
$MAPE_{fit}$			1.7238		1.7239		1.3787		1.1745		1.3752		0.9164		0.8120		0.9202		**0.7754**
17	9161.91	9700.85	538.95	9702.07	540.17	9457.35	295.44	9156.04	-5.87	9457.63	295.72	9223.72	61.82	9349.39	187.49	9335.55	173.64	9193.07	31.16
18	9300.64	10091.17	790.53	10092.36	791.71	9760.89	460.25	9352.44	51.80	9762.26	461.62	9436.66	136.02	9578.85	278.21	9565.95	265.31	9307.55	6.90
19	9184.37	10497.19	1312.82	10498.34	1313.97	10070.61	886.24	9540.61	356.24	10073.28	888.91	9643.71	459.34	9800.84	616.47	9790.72	606.35	9376.98	192.61
20	8948.80	10919.54	1970.75	10920.65	1971.86	10386.87	1438.07	9720.88	772.08	10391.06	1442.26	9845.29	896.49	10015.60	1066.80	10010.20	1061.41	9395.88	447.09
21	8245.59	11358.89	3113.31	11359.96	3114.37	10710.00	2464.42	9893.54	1647.95	10715.95	2470.36	10041.77	1796.19	10223.38	1977.79	10224.74	1979.16	9358.34	1112.76
22	8680.18	11815.92	3135.74	11816.93	3136.75	11040.35	2360.16	10058.89	1378.71	11048.29	2368.10	10233.49	1553.31	10424.39	1744.21	10434.64	1754.45	9258.01	577.83
23	9450.02	12291.34	2841.31	12292.29	2842.27	11378.22	1928.19	10217.23	767.20	11388.40	1938.38	10420.75	970.73	10618.87	1168.85	10640.16	1190.13	9088.04	-361.98
$MAPE_{pre}$			22.0926		22.1048		15.9107		8.1593		15.9628		9.5867		11.4457		11.4314		**4.4986**

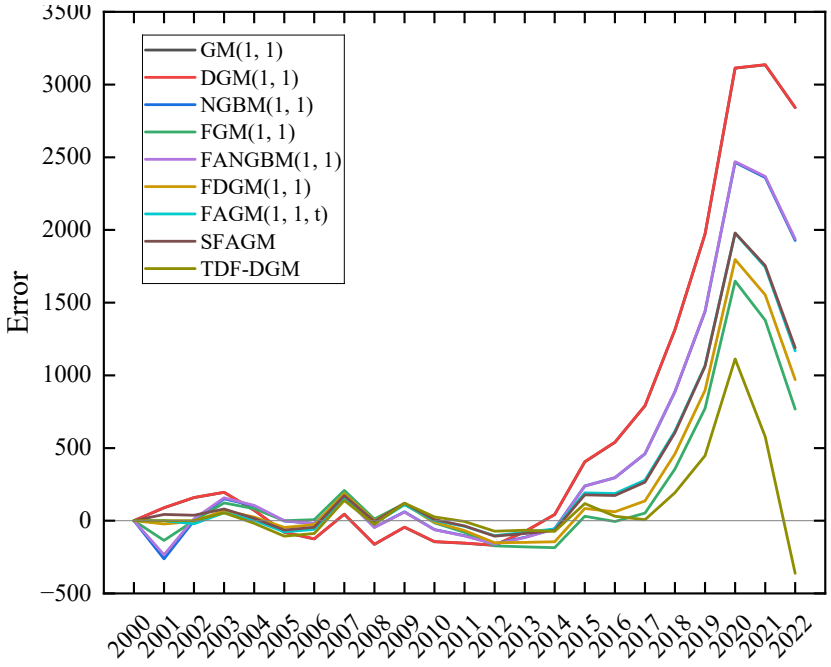

Figure 8. Optimal $MAPE_{fit}$ of model in Case III under PSO algorithm.

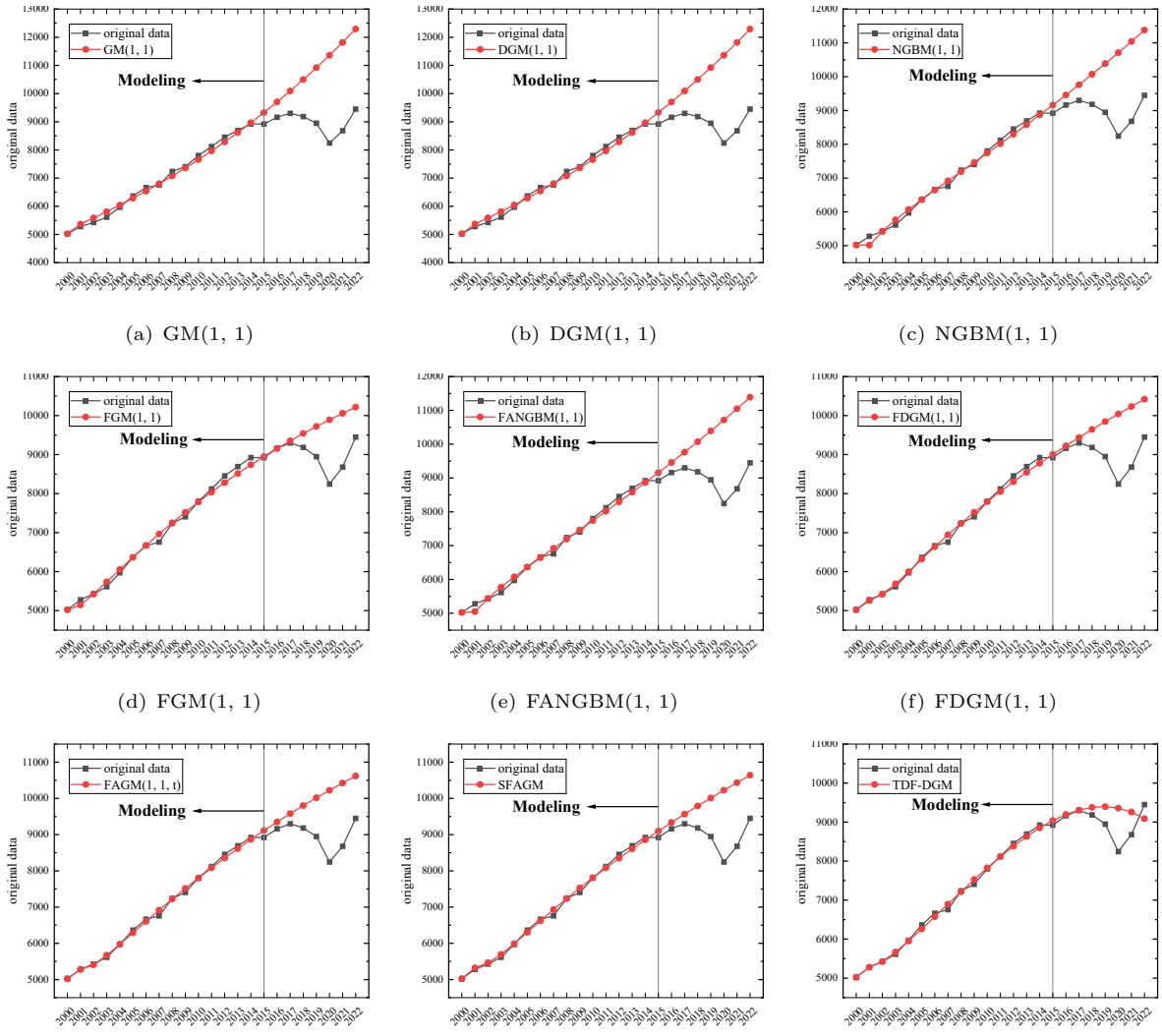

(a) GM(1, 1) (b) DGM(1, 1) (c) NGBM(1, 1)

(d) FGM(1, 1) (e) FANGBM(1, 1) (f) FDGM(1, 1)

(g) FAGM(1, 1, t^{α}) (h) SFAGM(1, 1) (i) TDF-DGM

Figure 9. Predicted values of all models in Case III.

3.4 Discussions

From the in-depth discussion of the three cases, it is evident that the TDF-DGM model consistently maintains a close relationship with the original data. Regardless of in-sample fitting or out-of-sample prediction, its performance consistently surpasses other models. Below, we will provide a more detailed analysis of the predictive capabilities and actual performance of this model.

In these three cases, compared to other linear grey system models, the TDF-DGM model demonstrates superior predictive performance both in-sample and out-of-sample, showing the lowest fitting errors and prediction errors. This indicates the TDF-DGM model's significant advantage in maintaining good predictive performance, especially in out-of-sample predictions.

Compared to linear grey system models, the TDF-DGM model not only exhibits stronger generalization capabilities but also provides more accurate predictive performance, offering reliable support for practical applications. In contrast to nonlinear grey system models, the TDF-DGM model's errors remain relatively stable at each data point, avoiding sudden large errors, which is a notable advantage. Interestingly, for data with certain volatility characteristics, the TDF-DGM

model always manages to capture trends more accurately, making the prediction results closer to the original data, a feat other competing models struggle to achieve.

Therefore, the TDF-DGM model excels in out-of-sample predictive performance, particularly in terms of stability and adaptability to volatile data. This makes the TDF-DGM model a powerful tool in practical applications, providing a solid foundation for accurate predictions and decision-making.

4 Conclusions

In this study, the time-delayed fractional discrete grey model with multiple fractional order (TDF-DGM) is employed to forecast oil consumption and production totals in the Asia-Pacific, Commonwealth of Independent States (CIS) and Middle East regions. Evaluating model performance using the Mean Absolute Percentage Error (MAPE), we compare eight different grey models and optimized their parameters using Particle Swarm Optimization (PSO) algorithm. Our analysis and comparison of oil production and consumption data across these regions demonstrate that the TDF-DGM model exhibits significant advantages in both fitting and forecasting capabilities. It shows the lowest fitting errors during the fitting phase and the smallest forecasting errors during the prediction phase, underscoring its effectiveness and reliability in predicting oil production and consumption data. These findings highlight the potential of the TDF-DGM model in addressing challenges in forecasting complex time-series data, offering robust support and guidance for future research and practical applications.

Reference

[1] Julong Deng. Control problems of grey systems. *Systems & Control Letters*, 1(5):288–294, 1982.

[2] Naiming Xie and Sifeng Liu. Discrete GM(1, 1) and mechanism of grey forecasting model. *Systems Engineering-Theory & Practice*, 25(1):93–99, 2005.

[3] Naiming Xie and Sifeng Liu. Research on extension of discrete grey model and its optimize formula. *Systems Engineering-Theory & Practice*, 26(6):108–112, 2006.

[4] Naiming Xie and Sifeng Liu. Discrete grey forecasting model and its optimization. *Applied mathematical modelling*, 33(2):1173–1186, 2009.

[5] Lifeng Wu, Sifeng Liu, Ligen Yao, Shuli Yan, and Dinglin Liu. Grey system model with the fractional order accumulation. *Communications in Nonlinear Science and Numerical Simulation*, 18(7):1775–1785, 2013.

[6] Naiming Xie, Sifeng Liu, Yingjie Yang, and Chaoqing Yuan. On novel grey forecasting model based on non-homogeneous index sequence. *Applied Mathematical Modelling*, 37(7):5059–5068, 2013.

[7] Zhengxin Wang, Qin Li, and Lingling Pei. Grey forecasting method of quarterly hydropower production in China based on a data grouping approach. *Applied Mathematical Modelling*, 51:302–316, 2017.

[8] Wuyong Qian and Aodi Sui. A novel structural adaptive discrete grey prediction model and its application in forecasting renewable energy generation. *Expert Systems with Applications*, 186:115761, 2021.

[9] Xin Ma and Zhibin Liu. Application of a novel time-delayed polynomial grey model to predict the natural gas consumption in China. *Journal of Computational and Applied Mathematics*, 324:17–24, 2017.

[10] Bo Zeng, Huiming Duan, Yun Bai, and Wei Meng. Forecasting the output of shale gas in China using an unbiased grey model and weakening buffer operator. *Energy*, 151:238–249, 2018.

[11] Xin Ma, Yisheng Hu, and Zhibin Liu. A novel kernel regularized nonhomogeneous grey model and its applications. *Communications in Nonlinear Science and Numerical Simulation*, 48:51–62, 2017.

[12] Faheemullah Shaikh, Qiang Ji, Pervez Hameed Shaikh, Nayyar Hussain Mirjat, and Muhammad Aslam Uqaili. Forecasting China' s natural gas demand based on optimised nonlinear grey models. *Energy*, 140:941–951, 2017.

[13] Qiang Wang and Xiaoxin Song. Forecasting China's oil consumption: a comparison of novel nonlinear-dynamic grey model (GM), linear GM, nonlinear GM and metabolism GM. *Energy*, 183:160–171, 2019.

[14] Chun-I Chen, Hong Long Chen, and Shuo-Pei Chen. Forecasting of foreign exchange rates of Taiwan' s major trading partners by novel nonlinear grey Bernoulli model NGBM(1, 1). *Communications in Nonlinear Science and Numerical Simulation*, 13(6):1194–1204, 2008.

[15] ZX Wang. GM(1, 1) power model with time-varying parameters and its application. *Control Decis*, 29(10):1828–1832, 2014.

[16] Paul Gatabazi, Jules Clement Mba, and Edson Pindza. Fractional gray Lotka-Volterra models with application to cryptocurrencies adoption. *Chaos: An Interdisciplinary Journal of Nonlinear Science*, 29(7), 2019.

[17] Xinping Xiao and Huiming Duan. A new grey model for traffic flow mechanics. *Engineering Applications of Artificial Intelligence*, 88:103350, 2020.

[18] Qinzi Xiao, Mingyun Gao, Xinping Xiao, and Mark Goh. A novel grey Riccati–Bernoulli model and its application for the clean energy consumption prediction. *Engineering Applications of Artificial Intelligence*, 95:103863, 2020.

[19] Wenqing Wu, Xin Ma, Bo Zeng, Yuanyuan Zhang, and Wanpeng Li. Forecasting short-term solar energy generation in Asia Pacific using a nonlinear grey Bernoulli model with time power term. *Energy & Environment*, 32(5):759–783, 2021.

[20] Xilin Luo, Huiming Duan, and Kai Xu. A novel grey model based on traditional Richards model and its application in COVID-19. *Chaos, Solitons & Fractals*, 142:110480, 2021.

[21] Wenqing Wu, Xin Ma, Yong Wang, Wei Cai, and Bo Zeng. Predicting China' s energy consumption using a novel grey Riccati model. *Applied Soft Computing*, 95:106555, 2020.

[22] Lifeng Wu, Sifeng Liu, Ligen Yao, Shuli Yan, and Dinglin Liu. Grey system model with the fractional order accumulation. *Communications in Nonlinear Science and Numerical Simulation*, 18(7):1775–1785, 2013.

[23] Wenqing Wu, Xin Ma, Bo Zeng, Yong Wang, and Wei Cai. Forecasting short-term renewable energy consumption of China using a novel fractional nonlinear grey Bernoulli model. *Renewable Energy*, 140:70–87, 2019.

[24] Yu Hu, Xin Ma, Wanpeng Li, Wenqing Wu, and Daoxing Tu. Forecasting manufacturing industrial natural gas consumption of China using a novel time-delayed fractional grey model with multiple fractional order. *Computational and Applied Mathematics*, 39:1–30, 2020.

[25] Xin Ma, Mei Xie, Wenqing Wu, Xinxing Wu, and Bo Zeng. A novel fractional time delayed grey model with Grey Wolf Optimizer and its applications in forecasting the natural gas and coal consumption in Chongqing China. *Energy*, 178:487–507, 2019.

[26] Nai ming Xie and Si feng Liu. Discrete grey forecasting model and its optimization. *Applied Mathematical Modelling*, 33(2):1173–1186, 2009.

[27] Chun-I Chen, Hong Long Chen, and Shuo-Pei Chen. Forecasting of foreign exchange rates of Taiwan' s major trading partners by novel nonlinear grey Bernoulli model NGBM(1,1). *Communications in Nonlinear Science and Numerical Simulation*, 13(6):1194–1204, 2008.

[28] Wei Meng, Daoli Yang, and Hui Huang. Prediction of China' s sulfur dioxide emissions by discrete grey model with fractional order generation operators. *Complexity*, 2018:1–13, 2018.

[29] Wenqing Wu, Xin Ma, Yuanyuan Zhang, Yong Wang, and Xinxing Wu. Analysis of novel FAGM (1, 1, t^{α}) model to forecast health expenditure of China. *Grey Systems: Theory and Application*, 9(2):232–250, 2019.

[30] Jie Xia, Xin Ma, and Wenqing Wu. FAGM(1,1) model based on Simpson formula and its application. *Chinese Management Science*, 29(05):240–248, 2021.